PERSPECTIVE

How to Cite: Gorbikova, E. (2026). Following Protons through Cytochrome c Oxidase by Infrared Spectroscopy: Current Results and Research Prospects. Contig, 1(3), 202616. DOI: 10.66273/3134-6359.2026.1.3.004

UDC: 577.152.1:543.422.4

Received: 15/09/2026 | Accepted: 04/10/2026 | Published online: 04/10/2026

Following Protons through Cytochrome *c* Oxidase by Infrared Spectroscopy: Current Results and Research Prospects

Elena Gorbikova*

University of Helsinki, Helsinki, Finland

* Corresponding author: elena.gorbikova@helsinki.fi | ORCID: 0000-0002-6078-6012

Abstract

Cytochrome *c* oxidase (CcO) couples the reduction of O_2 to water with proton pumping across the membrane, but the protonation events that link the two processes are only partly resolved. This Perspective summarises a series of static and time-resolved ATR-FTIR studies of the aa_3-type CcO from *Paracoccus denitrificans* published between 2006 and 2020 and places them in the context of recent structural and spectroscopic work. The FTIR studies assigned infrared signatures to the four redox centres, provided strong evidence that the cross-linked Tyr-280 is the proton donor for O–O bond scission, followed its protonation state around the catalytic cycle, resolved deprotonation and reprotonation of Glu-278 during the oxygen reaction, and provided infrared evidence consistent with a proton-loading site made up of several groups. Three developments make it timely to return to these questions: damage-free and cryo-EM structures of catalytic intermediates, single-shot microsecond infrared spectroscopy, and quantitative electrostatic and QM/MM models. Five research directions are proposed, each tied to a specific unresolved observation.

Keywords: cytochrome *c* oxidase; proton pumping; FTIR difference spectroscopy; time-resolved infrared spectroscopy; cross-linked tyrosine; proton-loading site; *Paracoccus denitrificans*

1. Introduction

Cytochrome *c* oxidase (CcO, complex IV) is the terminal enzyme of the respiratory chain in mitochondria and many aerobic bacteria. Electrons from cytochrome *c* pass through Cu_A and heme *a* to the binuclear centre (BNC) formed by heme a_3 and Cu_B, where O_2 is reduced to water. For every electron, one proton is consumed in this chemistry and a second is pumped across the membrane [1,2]. In A-type oxidases, protons enter from the negatively charged side of the membrane through the D- and K-channels. Mutagenesis of the yeast mitochondrial enzyme indicates that the D-channel carries the pumped protons there as it does in bacteria [3], although a role for the H-channel is still argued for the bovine enzyme [4].

The catalytic cycle runs through the intermediates R, A, P, F, O and E [1,5]. Electron transfer and oxygen chemistry in this cycle are comparatively well described. What is still incomplete is a time-ordered account of which groups carry the protons at each step. Infrared difference spectroscopy is one

of the few methods that report directly on the protonation and hydrogen bonding of individual groups in a working protein [6].

Between 2006 and 2020, a series of attenuated total reflection (ATR) FTIR studies of the aa_3-type CcO from *Paracoccus denitrificans* addressed this problem [7–14]. This Perspective summarises what those studies established (Section 2, Table 1 and Figure 1), sets out what they left open in the light of later work (Section 3) and proposes directions for further research (Section 4). Residue numbers refer to the *P. denitrificans* enzyme unless stated otherwise.

2. What the FTIR Studies Established

2.1 Equilibrium Spectra

Electrochemical redox titrations followed by ATR-FTIR sorted most of the infrared difference bands into four groups, one for each redox centre [7]. Twelve bands titrated with the highest midpoint potential (412 mV at pH 6.5, with a slope of 52 mV per pH unit in the alkaline range) and were linked to Cu_B. Bands with a pH-independent potential of 250 mV were assigned to Cu_A. The two hemes had almost equal potentials (359 and 350 mV at pH 8.0) and a strong negative redox interaction (−115 mV). The band shift of protonated Glu-278 at 1737/1746 cm^{-1} followed the redox state of heme *a*. A study over the range pH 5.2–9.5 then showed two pH-dependent processes in the reduced-minus-oxidised spectrum, with apparent pK_a values of 6.6 and 8.4, and a sharp O–H band of an asymmetrically hydrogen-bonded water molecule that appears on reduction [8].

2.2 Time-Resolved Spectra of the Oxygen Reaction

A flow-flash chamber on the ATR prism allowed the reaction of the fully reduced, CO-inhibited enzyme with O_2 to be repeated many times on one protein film and recorded in rapid-scan mode [9]. In the D124N variant, where the entrance of the D-channel is blocked, this showed deprotonation of Glu-278 on formation of F (trough at 1735 cm^{-1}) and its reprotonation in the F→O step (1743 cm^{-1}), which the mutation makes rate-limiting [9].

In the E278Q variant the reaction stops at the P_R intermediate. Its formation, in about 60 µs, was accompanied by a band at 1308 cm^{-1} characteristic of the deprotonated cross-linked Tyr-280 and by an electrometric signal equivalent to proton movement over about 4 Å. These results strongly supported Tyr-280 as the proton donor for O–O bond scission [10]. Following the same band through the rest of the cycle showed that the tyrosine stays fully deprotonated in F (pK_a below about 5.5), has a pK_a of about 6.6 in O whether that state is reached kinetically or at equilibrium, and, as inferred from equilibrium redox titrations, is fully reprotonated in the O→E step together with reduction of Cu_B [11].

2.3 The Proton-Loading Site

The N131V and D124N enzymes do not pump protons, yet they show a fast electrogenic phase that is too large for proton transfer to the BNC alone. It was attributed to loading of the proton-loading site (PLS) above the hemes, with a conserved D-channel tyrosine (Tyr-35) as a possible internal donor, followed by return of the proton to the BNC [12]. The infrared counterpart was reported in 2020: seven bands are present in the unresolved fast phase of both variants, reappear with opposite sign in the slow phase and are absent, or within the noise, in E278Q [14]. Some of them should therefore reflect protonation of the PLS. The band near 1699 cm^{-1} was attributed to a partially protonated A-propionate of heme a_3, and bands at 1096 and 1107 cm^{-1} in the double-difference spectra to a histidine, possibly His-403. Protonated water clusters were considered the most probable further contributor, although their weak absorbance could not be seen in this window. This agrees with electrostatic and multiscale calculations that describe the PLS as a cluster of groups, or as a protonated water cluster, rather than a single residue [15,16].

2.4 Oxidised States

The oxidised enzyme exists in a relaxed form (O) and in a metastable form (O_H) that is produced by oxidation of the reduced enzyme, and only reduction of O_H is coupled to proton pumping [17]. Static O→R spectra of the wild-type enzyme and time-resolved R→O spectra of the wild-type, N131V and D124N enzymes, recorded at acidic and alkaline pH (D124N at pH 9.0 only), were indistinguishable between 1800 and 1000 cm^{-1} [13]. Any structural difference between the two forms therefore lies outside this window or below the detection limit of those measurements.

Table 1. ATR-FTIR studies of cytochrome *c* oxidase from *Paracoccus denitrificans* summarised in this Perspective.

Reference, year	Approach	Enzyme form	Main result
[7], 2006	Electrochemical redox titration followed by ATR-FTIR	Wild type	Infrared bands grouped by redox centre. E_m: Cu_B 412 mV (pH 6.5); Cu_A 250 mV; heme *a* 359 mV and heme a_3 350 mV (pH 8.0); heme–heme interaction −115 mV
[8], 2007	Reduced-minus-oxidised spectra, pH 5.2–9.5; D_2O and $H_2{}^{18}O$ exchange	Wild type	Two protolytic processes (pK_a 6.6 and 8.4); O–H band of a water molecule appears on reduction
[9], 2007	Flow-flash rapid-scan ATR-FTIR of the O_2 reaction	D124N	Glu-278 deprotonates on formation of F and is reprotonated in F→O
[10], 2008	Time-resolved optical, FTIR and electrometric measurements	E278Q	Strong evidence that the cross-linked Tyr-280 donates the proton for O–O bond scission (1308 cm^{-1}; about 60 μs; about 4 Å)
[11], 2008	Time-resolved and equilibrium FTIR	N131V, wild type	Tyr-280 deprotonated in F (pK_a < 5.5); pK_a ≈ 6.6 in O; reprotonation at O→E with Cu_B reduction inferred from equilibrium titrations
[12], 2010	Time-resolved optical, FTIR and electrometric measurements	D124N, D124N/Y35F, N131V	Non-pumping variants still load the PLS; Tyr-35 proposed as internal proton donor
[13], 2020	Static O→R (wild type) and time-resolved R→O FTIR, pH 6.0–9.0	Wild type, N131V, D124N	No difference between O and O_H at 1800–1000 cm^{-1}
[14], 2020	Flow-flash rapid-scan ATR-FTIR; double-difference spectra	N131V, D124N, E278Q	Seven bands meet the criteria for PLS protonation; candidates are the heme a_3 A-propionate (about 1699 cm^{-1}), His-403 (1096 and 1107 cm^{-1}) and water

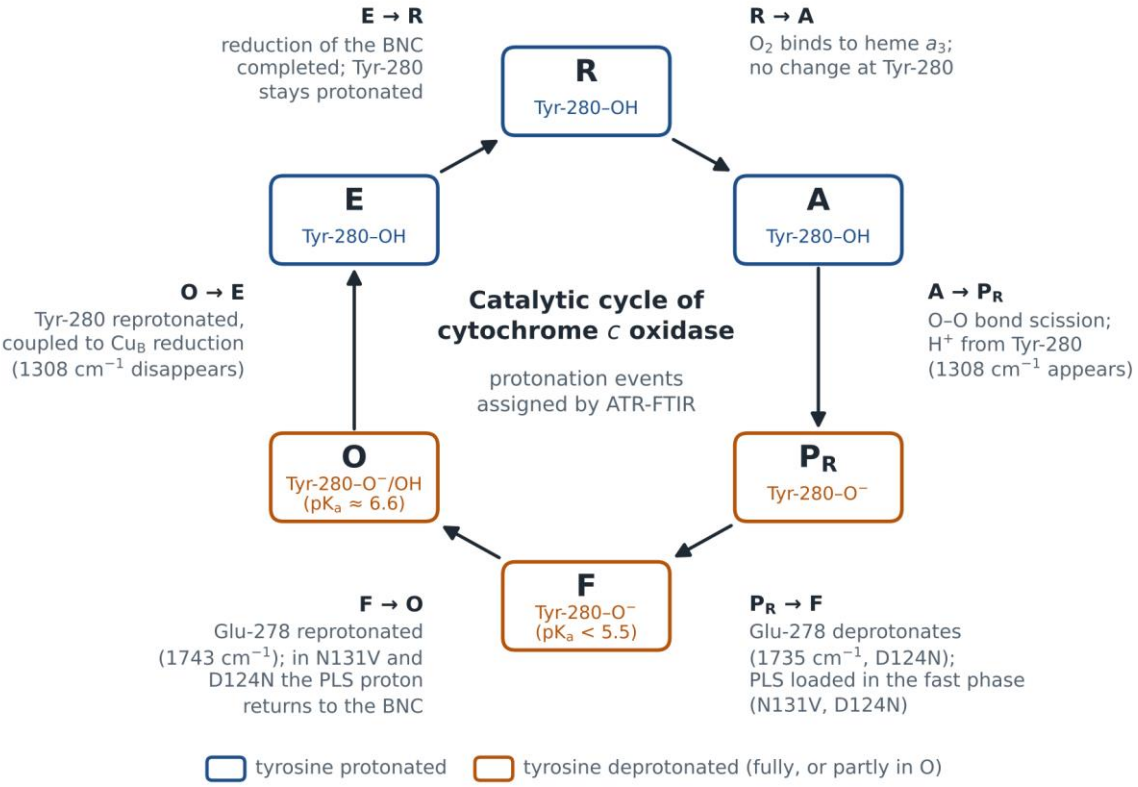


Figure 1. Protonation events in the catalytic cycle of cytochrome *c* oxidase from *Paracoccus denitrificans* assigned by ATR-FTIR spectroscopy. Boxes show the intermediates and the protonation state of the cross-linked Tyr-280 [10,11]. Glu-278 changes were resolved in the D124N variant [9]; loading of the proton-loading site (PLS) was inferred for the non-pumping N131V and D124N variants [12,14]. BNC, binuclear centre.

3. Open Questions

Four limitations of the work summarised above define what should be done next.

The O and O_H states. Serial femtosecond crystallography and resonance Raman spectroscopy of bovine CcO indicate that the relaxed O state has hydroxide on heme a_3 and water on Cu_B, as in O_H, but a neutral protonated cross-linked tyrosine, whereas the tyrosine is taken to be a tyrosinate in O_H [18]. A cryo-EM study of the *P. denitrificans* enzyme at up to 1.9 Å resolution instead interpreted the active-site density of the O state as a peroxide dianion and proposed a revised cycle [19]. X-ray structures of the bovine O and E forms add further detail [20], and the structures of the intermediates have been reviewed against time-resolved spectroscopic, structural and computational evidence [5]. The infrared data gave the same tyrosine pK_a in kinetically resolved and equilibrium O [11] and no fingerprint difference between O and O_H [13]. These results are not necessarily in conflict, because the species, the pH and the time after oxidation differ and O_H relaxes on a time scale of seconds to tens of seconds [5,18], but they have not been reconciled.

The electronic state of the tyrosine. Magnetic circular dichroism and X-ray absorption data on the F intermediate were recently interpreted as an electron-delocalised copper–tyrosyl radical state that recurs in all four proton-pumping intermediates [21]. How this description relates to the 1308 cm^{-1} band, which was assigned to a tyrosinate in P_R, F and O [10,11], has not been examined.

Time resolution. Rapid-scan FTIR resolved events slower than about 46 ms. The phase in which the PLS is loaded appears only as an unresolved step, and the evidence for it comes from non-pumping variants measured at 0 °C [14]. In the proton-pumping enzyme, electrometry places loading of the pump site at about 150 µs and release of the proton at about 2.6 ms after electron injection [22].

Spectral window and assignment. The time-resolved data cover only 1800–1000 cm^{-1}. The assignment of the PLS bands to a propionate and to His-403 rests on band positions alone, without isotope labelling or mutation of the candidate groups [14]. The region above 3500 cm^{-1}, where weakly hydrogen-bonded internal water molecules absorb [8,23], has not been studied in time-resolved mode.

4. Research Prospects

4.1 Microsecond Infrared Spectroscopy of a Non-Repetitive Reaction

Step-scan FTIR needs a reaction that can be repeated many hundreds to thousands of times under identical conditions. This is hard to achieve for the flow-flash oxygen reaction on a protein film, where every cycle requires re-reduction of the enzyme and rebinding of CO. Dual-comb spectrometers based on quantum cascade lasers (QCL) record spectra and kinetics from a single excitation with sub-microsecond to microsecond resolution [24,25]. A femtosecond mid-infrared facility has already detected protonation of a carboxyl group in bovine CcO under turnover within 1 ms [26], and time-resolved infrared work on the *Cereibacter sphaeroides* enzyme resolved deprotonation of the Glu-278 equivalent in 13 µs after transient reduction of heme *a* [27]. Applying these methods to the *P. denitrificans* flow-flash system would resolve PLS loading and release in the wild-type enzyme at the marker positions already identified: about 1700 cm^{-1} for the propionate, about 1100 cm^{-1} for histidine, 1308 cm^{-1} for Tyr-280 and about 1740 cm^{-1} for Glu-278. The spectral coverage of a single-shot measurement is narrow (55 cm^{-1} in [24]), so each marker region has to be recorded separately.

4.2 Water and the High-Frequency Region

Extending time-resolved measurements to 4000–2000 cm^{-1} would test two specific proposals. The first is that the PLS is a protonated water cluster [16]; in bacteriorhodopsin such a cluster gives a broad continuum absorbance rather than sharp bands [28]. The second is that O and O_H differ in water molecules at or near the BNC [13,18]. Equilibrium spectra of bovine CcO already resolve several weakly hydrogen-bonded water molecules that respond to redox and ligand changes [23], and D_2O and $H_2{}^{18}O$ exchange, as used in [8], provides the assignment.

4.3 Assignments That Do Not Rest on Band Position

The PLS assignment needs variants at His-403 and Asp-399 and specific isotope labelling of histidine and of the heme propionates. Computation is the second route. Quantum chemical and QM/MM models now give electric fields and proton-transfer energetics around the PLS [29], and the stretching frequency of CO bound to heme a_3 has been used as a vibrational Stark probe of field changes at the BNC [30]. Difference spectra calculated for specific protonation patterns of the propionate–histidine–water cluster could be compared directly with the double-difference spectra in [14].

4.4 Connecting Infrared Data to Structures of Intermediates

The disagreement over O and O_H (Section 3) can be tested with a simple experiment: follow the 1308 cm^{-1} tyrosinate band and the water region from milliseconds to minutes after oxidation, at several pH values, in the bacterial enzyme and in a mitochondrial one. The yeast enzyme is suited to this because it can be mutated and its redox FTIR spectra have been compared with those of the bovine and *P. denitrificans* enzymes [3,31]. Time-resolved crystallography has captured an oxygen intermediate of bovine CcO [32], photolabile caged-oxygen compounds are being developed to start the reaction in

microcrystals [33], and time-resolved infrared microspectroscopy of protein microcrystals has been established [34]. Oxidation in the dark by controlled gas exchange removes the need for CO photolysis [35].

4.5 Membrane Potential and Native-Like Environments

All the infrared work summarised here used detergent-depleted films without a membrane potential. The 2008 analysis predicted that a potential of 180 mV would lower the pK_a of Tyr-280 by about two units [11]; this has not been tested. Lipid nanodiscs provide a defined bilayer that is compatible with FTIR difference spectroscopy of CcO [36] and are a first step towards measurements on energised membranes.

Table 2. Open questions and proposed infrared experiments.

Open question	Proposed experiment	Infrared readout
When is the PLS loaded and released in the wild-type enzyme?	Single-shot QCL dual-comb spectroscopy of the flow-flash reaction, microseconds to milliseconds, one marker region at a time	About 1700 cm^{-1} (propionate); about 1100 cm^{-1} (histidine); 1308 cm^{-1} (Tyr-280); about 1740 cm^{-1} (Glu-278)
Does a protonated water cluster contribute to the PLS?	Time-resolved spectra at 4000–2000 cm^{-1} with D_2O and $H_2{}^{18}O$ exchange	Continuum absorbance; O–H stretch of weakly hydrogen-bonded water (3560–3800 cm^{-1})
Which groups give the PLS bands?	His-403 and Asp-399 variants; isotope-labelled histidine and heme propionates; QM/MM-calculated difference spectra	Shift or loss of bands in the double-difference spectra of [14]
How do O and O_H differ?	Time (milliseconds to minutes) and pH series after oxidation; bacterial and mitochondrial enzymes	1308 cm^{-1} (Tyr-280); water region
How does membrane potential change the protonation of Tyr-280?	Enzyme in nanodiscs or proteoliposomes under an imposed potential	1308 cm^{-1} as a function of potential and pH

5. Conclusions

The FTIR studies of *P. denitrificans* CcO assigned protonation changes of Tyr-280 and Glu-278 to individual steps of the catalytic cycle and gave time-resolved infrared data on the PLS. Their limits were set by the technology of the time: millisecond resolution, a single spectral window and assignments based on band position. Single-shot microsecond infrared methods, damage-free structures of intermediates and quantitative calculations now address each of these limits. The most direct next experiments are microsecond infrared kinetics of the wild-type oxygen reaction, time-resolved spectra in the water region, and a time and pH series of the tyrosine band across the $O_H \rightarrow O$ relaxation.

Abbreviations

ATR, attenuated total reflection; BNC, binuclear centre; CcO, cytochrome *c* oxidase; FTIR, Fourier transform infrared; PLS, proton-loading site; QCL, quantum cascade laser; QM/MM, quantum mechanics/molecular mechanics.

Data Availability Statement

No new data were created or analysed in this work.

Author Contributions

Conceptualization, Investigation, and Writing: E.A.G.

Acknowledgments

We warmly thank Dr. Nikolai Belevich for excellent technical assistance and Dr. Timur Nikitin for critical reading of the manuscript.

Funding

EG was supported by the Center of International Mobility (CIMO) and the Informational and Structural Biology (ISB) Graduate School. The work was supported by the Sigrid Jusélius Foundation, Biocentrum Helsinki and the Academy of Finland (project numbers 200726, 44895, and 115108).

Ethics approval and consent

Not applicable.

Competing Interests

The authors declare that the research was conducted in the absence of any commercial or financial relationships that could be construed as a potential conflict of interest.

References

1. Wikström M, Krab K, Sharma V (2018) Oxygen activation and energy conservation by cytochrome *c* oxidase. *Chemical Reviews* 118 (5):2469-2490. DOI: 10.1021/acs.chemrev.7b00664
2. Kaila VRI, Verkhovsky MI, Wikström M (2010) Proton-coupled electron transfer in cytochrome oxidase. *Chemical Reviews* 110 (12):7062-7081. DOI: 10.1021/cr1002003
3. Maréchal A, Xu JY, Genko N, Hartley AM, Haraux F, Meunier B, Rich PR (2020) A common coupling mechanism for A-type heme-copper oxidases from bacteria to mitochondria. *Proceedings of the National Academy of Sciences USA* 117 (16):9349-9355. DOI: 10.1073/pnas.2001572117
4. Shimada A, Tsukihara T, Yoshikawa S (2023) Recent progress in experimental studies on the catalytic mechanism of cytochrome *c* oxidase. *Frontiers in Chemistry* 11:1108190. DOI: 10.3389/fchem.2023.1108190
5. Wikström M, Gennis RB, Rich PR (2023) Structures of the intermediates in the catalytic cycle of mitochondrial cytochrome *c* oxidase. *Biochimica et Biophysica Acta – Bioenergetics* 1864 (2):148933. DOI: 10.1016/j.bbabio.2022.148933
6. Lorenz-Fonfria VA (2020) Infrared difference spectroscopy of proteins: from bands to bonds. *Chemical Reviews* 120 (7):3466-3576. DOI: 10.1021/acs.chemrev.9b00449

7. Gorbikova EA, Vuorilehto K, Wikström M, Verkhovsky MI (2006) Redox titration of all electron carriers of cytochrome *c* oxidase by Fourier transform infrared spectroscopy. *Biochemistry* 45 (17):5641-5649. DOI: 10.1021/bi060257v
8. Gorbikova EA, Belevich NP, Wikström M, Verkhovsky MI (2007) Protolytic reactions on reduction of cytochrome *c* oxidase studied by ATR-FTIR spectroscopy. *Biochemistry* 46 (13):4177-4183. DOI: 10.1021/bi602523a
9. Gorbikova EA, Belevich NP, Wikström M, Verkhovsky MI (2007) Time-resolved ATR-FTIR spectroscopy of the oxygen reaction in the D124N mutant of cytochrome *c* oxidase from *Paracoccus denitrificans*. *Biochemistry* 46 (45):13141-13148. DOI: 10.1021/bi701614w
10. Gorbikova EA, Belevich I, Wikström M, Verkhovsky MI (2008) The proton donor for O–O bond scission by cytochrome *c* oxidase. *Proceedings of the National Academy of Sciences USA* 105 (31):10733-10737. DOI: 10.1073/pnas.0802512105
11. Gorbikova EA, Wikström M, Verkhovsky MI (2008) The protonation state of the cross-linked tyrosine during the catalytic cycle of cytochrome *c* oxidase. *Journal of Biological Chemistry* 283 (50):34907-34912. DOI: 10.1074/jbc.M803511200
12. Belevich I, Gorbikova E, Belevich NP, Rauhamäki V, Wikström M, Verkhovsky MI (2010) Initiation of the proton pump of cytochrome *c* oxidase. *Proceedings of the National Academy of Sciences USA* 107 (43):18469-18474. DOI: 10.1073/pnas.1010974107
13. Gorbikova E, Kalendar R (2020) Comparison between O and OH intermediates of cytochrome *c* oxidase studied by FTIR spectroscopy. *Frontiers in Chemistry* 8:387. DOI: 10.3389/fchem.2020.00387
14. Gorbikova E, Samsonov SA, Kalendar R (2020) Probing the proton-loading site of cytochrome *c* oxidase using time-resolved Fourier transform infrared spectroscopy. *Molecules* 25 (15):3393. DOI: 10.3390/molecules25153393
15. Lu J, Gunner MR (2014) Characterizing the proton loading site in cytochrome *c* oxidase. *Proceedings of the National Academy of Sciences USA* 111 (34):12414-12419. DOI: 10.1073/pnas.1407187111
16. Supekar S, Gamiz-Hernandez AP, Kaila VRI (2016) A protonated water cluster as a transient proton-loading site in cytochrome *c* oxidase. *Angewandte Chemie International Edition* 55 (39):11940-11944. DOI: 10.1002/anie.201603606
17. Bloch D, Belevich I, Jasaitis A, Ribacka C, Puustinen A, Verkhovsky MI, Wikström M (2004) The catalytic cycle of cytochrome *c* oxidase is not the sum of its two halves. *Proceedings of the National Academy of Sciences USA* 101 (2):529-533. DOI: 10.1073/pnas.0306036101
18. Ishigami I, Sierra RG, Su Z, Peck A, Wang C, Poitevin F, Lisova S, Hayes B, Moss FR, Boutet S, et al. (2023) Structural insights into functional properties of the oxidized form of cytochrome *c* oxidase. *Nature Communications* 14 (1):5752. DOI: 10.1038/s41467-023-41533-x
19. Kolbe F, Safarian S, Piórek Ż, Welsch S, Müller H, Michel H (2021) Cryo-EM structures of intermediates suggest an alternative catalytic reaction cycle for cytochrome *c* oxidase. *Nature Communications* 12 (1):6903. DOI: 10.1038/s41467-021-27174-y
20. Shimada A, Hara F, Shinzawa-Itoh K, Kanehisa N, Yamashita E, Muramoto K, Tsukihara T, Yoshikawa S (2021) Critical roles of the Cu_B site in efficient proton pumping as revealed by crystal structures of mammalian cytochrome *c* oxidase catalytic intermediates. *Journal of Biological Chemistry* 297 (5):100967. DOI: 10.1016/j.jbc.2021.100967
21. Jose A, Braun A, Hong S, Gennis RB, Solomon EI (2026) Spectroscopic elucidation of an electron-delocalized copper-tyrosine state in heme-copper oxidases reveals its role in proton pumping. *Proceedings of the National Academy of Sciences USA* 123 (2):e2602110123. DOI: 10.1073/pnas.2602110123
22. Belevich I, Bloch DA, Belevich N, Wikström M, Verkhovsky MI (2007) Exploring the proton pump mechanism of cytochrome *c* oxidase in real time. *Proceedings of the National Academy of Sciences USA* 104 (8):2685-2690. DOI: 10.1073/pnas.0608794104
23. Maréchal A, Rich PR (2011) Water molecule reorganization in cytochrome *c* oxidase revealed by FTIR spectroscopy. *Proceedings of the National Academy of Sciences USA* 108 (21):8634-8638. DOI: 10.1073/pnas.1019419108

24. Klocke JL, Mangold M, Allmendinger P, Hugi A, Geiser M, Jouy P, Faist J, Kottke T (2018) Single-shot sub-microsecond mid-infrared spectroscopy on protein reactions with quantum cascade laser frequency combs. *Analytical Chemistry* 90 (17):10494-10500. DOI: 10.1021/acs.analchem.8b02531
25. Norahan MJ, Horvath R, Woitzik N, Jouy P, Eigenmann F, Gerwert K, Kötting C (2021) Microsecond-resolved infrared spectroscopy on nonrepetitive protein reactions by applying caged compounds and quantum cascade laser frequency combs. *Analytical Chemistry* 93 (19):6779-6783. DOI: 10.1021/acs.analchem.1c00666
26. Li C, Nishiguchi T, Shinzawa-Itoh K, Yoshikawa S, Ogura T, Nakashima S (2018) Performance of a time-resolved IR facility for assessment of protonation states and polarity changes in carboxyl groups in a large membrane protein, mammalian cytochrome *c* oxidase, under turnover conditions in a sub-millisecond time resolution. *Biochimica et Biophysica Acta – Bioenergetics* 1859 (10):1045-1050. DOI: 10.1016/j.bbabio.2018.05.015
27. Baserga F, Langner P, Schubert L, Storm JP, Schlesinger R, Heberle J (2025) Proton-coupled electron transfer in cytochrome *c* oxidase: heme *a* controls the protonation dynamics of E286. *ChemPhysChem* 26:e202500539. DOI: 10.1002/cphc.202500539
28. Garczarek F, Gerwert K (2006) Functional waters in intraprotein proton transfer monitored by FTIR difference spectroscopy. *Nature* 439 (7072):109-112. DOI: 10.1038/nature04231
29. Saura P, Riepl D, Frey DM, Wikström M, Kaila VRI (2022) Electric fields control water-gated proton transfer in cytochrome *c* oxidase. *Proceedings of the National Academy of Sciences USA* 119 (38):e2207761119. DOI: 10.1073/pnas.2207761119
30. Baserga F, Dragelj J, Kozuch J, Mohrmann H, Knapp EW, Stripp ST, Heberle J (2021) Quantification of local electric field changes at the active site of cytochrome *c* oxidase by Fourier transform infrared spectroelectrochemical titrations. *Frontiers in Chemistry* 9:669452. DOI: 10.3389/fchem.2021.669452
31. Maréchal A, Hartley AM, Warelow TP, Meunier B, Rich PR (2018) Comparison of redox and ligand binding behaviour of yeast and bovine cytochrome *c* oxidases using FTIR spectroscopy. *Biochimica et Biophysica Acta – Bioenergetics* 1859 (9):705-711. DOI: 10.1016/j.bbabio.2018.05.018
32. Ishigami I, Lewis-Ballester A, Echelmeier A, Brehm G, Zatsepin NA, Grant TD, Coe JD, Lisova S, Nelson G, Zhang S, et al. (2019) Snapshot of an oxygen intermediate in the catalytic reaction of cytochrome *c* oxidase. *Proceedings of the National Academy of Sciences USA* 116 (9):3572-3577. DOI: 10.1073/pnas.1814526116
33. Sandelin E, Johannesson J, Wendt O, Brändén G, Neutze R, Wallentin CJ (2024) Characterization and evaluation of photolabile (μ-peroxo)(μ-hydroxo)bis[bis(bipyridyl)cobalt caged oxygen compounds to facilitate time-resolved crystallographic studies of cytochrome *c* oxidase. *Photochemical & Photobiological Sciences* 23 (5):839-851. DOI: 10.1007/s43630-024-00558-x
34. Sato W, Yamada D, Kubo M (2024) Time-resolved IR spectroscopy for monitoring protein dynamics in microcrystals. *Methods in Enzymology* 709:161-176. DOI: 10.1016/bs.mie.2024.10.006
35. Baserga F, Storm J, Schlesinger R, Heberle J, Stripp ST (2023) The catalytic reaction of cytochrome *c* oxidase probed by in situ gas titrations and FTIR difference spectroscopy. *Biochimica et Biophysica Acta – Bioenergetics* 1864 (4):149000. DOI: 10.1016/j.bbabio.2023.149000
36. Baserga F, Vorkas A, Crea F, Schubert L, Chen JL, Redlich A, La Greca M, Storm J, Oldemeyer S, Hoffmann K, et al. (2022) Membrane protein activity induces specific molecular changes in nanodiscs monitored by FTIR difference spectroscopy. *Frontiers in Molecular Biosciences* 9:915328. DOI: 10.3389/fmolb.2022.915328

Author Information

Full Name	Elena Gorbikova
Department	
Institution	University of Helsinki, Helsinki, Finland

Email	elena.gorbikova@helsinki.fi
ORCID	0000-0002-6078-6012
Scopus ID	